Luporini, P., Raffioni, S., Concetti, A., & Miceli, C. (1986) *Proc. Natl. Acad. Sci. U.S.A. 83*, 2889-2893.
Merril, C. R., Goldman, D., & Von Keuren, M. L. (1983) *Methods Enzymol. 96*, 230-239.
Miceli, C., Concetti, A., & Luporini, P. (1983) *Exp. Cell Res. 149*, 593-598.
Miceli, C., La Terza, A., & Melli, M. (1989) *Proc. Natl. Acad. Sci. U.S.A.* (in press).
Miyake, A. (1981) in *Biochemistry and Physiology of Protozoa* (Levandowsky, M., & Hutner, S. H., Eds.) Vol. 4, pp 125-198, Academic Press, New York.
Miyake, A., & Beyer, J. (1973) *Exp. Cell Res. 76*, 15-24.
Raffioni, S., Miceli, C., Concetti, A., Barra, D., & Luporini, P. (1987) *Exp. Cell Res. 172*, 417-424.
Raffioni, S., Luporini, P., Chait, B. T., Disper, S. S., & Bradshaw, R. A. (1988) *J. Biol. Chem. 263*, 18152-18159.
Reisfeld, R. A., Lewis V. J., & Williams, D. E. (1962) *Nature (London) 195*, 281-283.
Straus, D. S (1984) *Endocr. Rev. 5*, 356-369.
Wringley, C. W. (1971) *Methods Enzymol. 22*, 559-564.

Persistence of the α-Helix Stop Signal in the S-Peptide in Trifluoroethanol Solutions†

Jeffrey W. Nelson*
Department of Biochemistry, Louisiana State University, Baton Rouge, Louisiana 70803
Neville R. Kallenbach
Department of Chemistry, New York University, New York, New York 10003
Received December 5, 1988; Revised Manuscript Received March 8, 1989

ABSTRACT: α-Helix formation in the S-peptide (residues 1-19 of ribonuclease A) was studied in detail by use of two-dimensional ^{1}H nuclear magnetic resonance to monitor the effects of 2,2,2-trifluoroethanol (TFE) at 0 °C and pH* 2.07. TFE stabilizes the S-peptide α-helix. Helix formation by a particular amino acid was monitored by the chemical shifts of the C^α, C^β, and C^γ protons while increasing the concentration of TFE: large changes in chemical shift of a particular residue indicate that it is induced to go helical, whereas small chemical shift changes indicate little helix formation. Residues Thr-3 to Met-13 undergo chemical shift changes consistent with helix formation, whereas the other residues do not. Earlier work [Kim, P. S., & Baldwin, R. L. (1984) *Nature 307*, 329-334] reported that residues Thr-3 to His-12 become helical in aqueous solution. The existence of a "helix stop signal" was inferred from this behavior. We thus conclude that this helix stop signal persists in TFE solutions.

The S-peptide, residues 1-19 or 1-20 of RNase A,[1] forms an unusually stable α-helix in aqueous solution (Brown & Klee, 1971). Extensive studies on analogues of the C-peptide, residues 1-13 of RNase A, have shown that the stability depends on the charges of the amino acid side chains and helix termini (Shoemaker et al., 1987, 1985). This has been termed the "charged-group effect" and is determined by measuring the helix stability as the charges of the titratable side chains are altered by changing the pH, as well as by chemically introducing or removing charged side chains.

An NMR study indicated that only residues 3-12 of S-peptide-(1-20) become helical in aqueous solution (Kim & Baldwin, 1984). Because the last several residues of the S-peptide fail to become helical, they hypothesized the existence of a "helix stop signal" that terminates the helix near His-12. Standard helix-coil transition theory predicts that short helical segments are strongly cooperative and that, once nucleation is achieved, propagation of helix is facile.

It is well-known that the cosolvent 2,2,2-trifluoroethanol (TFE) stabilizes the S-peptide α-helix (Filippi et al., 1976, 1978). A circular dichroism study of the effects of pH*, temperature, and TFE concentration was reported by us previously (Nelson & Kallenbach, 1986). We discovered that the magnitude of the charged-group effect does not increase in TFE solutions, so that the difference in stability vs pH* is nearly the same at TFE concentrations up to 40 mol %. One difference is that in TFE solutions the helix does not become less stable as the pH* is reduced below about 3.8, as it does in aqueous solution. The titration curve of helix stability vs TFE concentration is cooperative at 0 °C, meaning that the helix stability increases greatly as the TFE concentration increases up to 10 mol % and then levels off. However, the cooperativity is much lower at temperatures between 50 and

†This work was supported by the National Institutes of Health under Grants GM 10840 and GM 31861 and by the U.S. Department of Energy, Office of Energy Research, under Contract 82 ER 60090. J.W.N. was supported by NIH Training Grant CA 09485 during the early part of the research and by an LSU Council on Research Summer Faculty Research Stipend during the later stages.
*Author to whom correspondence should be addressed.

[1] Abbreviations: TFE, 2,2,2-trifluoroethanol; TFE-d_3, fully deuterated TFE; RNase A, ribonuclease A; S-peptide-(1-19), residues 1-19 of RNase A; S-peptide-(1-20), residues 1-20 of RNase A; pH*, pH in solutions containing organic cosolvent; TSP, sodium 3-(trimethylsilyl)-propionate-*2,2,3,3-d*$_4$; NMR, nuclear magnetic resonance; 1D NMR, one-dimensional NMR; 2D NMR, two-dimensional NMR; FID, free induction decay; ppm, parts per million; DQF-COSY, double-quantum-filtered correlation spectroscopy; NOESY, nuclear Overhauser effect spectroscopy; RELAY, relayed coherence transfer spectroscopy; TPPI, time-proportional phase increments; $[\theta]_{222}$, mean residue ellipticity at 222 nm; Ala_3, tripeptide alanylalanylalanine.

0006-2960/89/0428-5256$01.50/0

75 °C (Nelson & Kallenbach, 1986). The effect of TFE on the thermal transition of the S-peptide α-helix has been studied by NMR (Rico et al., 1986). They found that the thermal transitions are broadened significantly in the presence of TFE.

In this study, we want to identify in detail which amino acids in S-peptide-(1–19) are induced to become helical when TFE is added to the solution. In particular, we want to determine whether the helix stop signal remains intact or if TFE induces the rest of the peptide to become helical. We have utilized 2D NMR in order to monitor the behavior of each individual amino acid during a TFE titration at 0 °C in 0.01 M HCl. This corresponds to a pH* of 2.07 and was chosen because the helix shows maximal stability at low pH* in TFE solutions (Nelson & Kallenbach, 1986). In 1D NMR spectra, one cannot follow the shifts due to spectral overlap, and we believe the 2D NMR method is essential in this kind of analysis. The proton resonances in 10 mol % TFE were assigned by use of DQF-COSY in D_2O and RELAY and NOESY in H_2O. The titration curves of the nonexchangeable protons were measured by DQF-COSY spectra at 0, 5, 10, 15, and 20 mol % TFE. The resonance positions changed smoothly and could be followed throughout the titration. We found that only residues Thr-3 to Met-13 exhibited significant chemical shift changes during the titration, indicating that the helix stop signal remains intact in TFE solutions up to 20 mol %.

Materials and Methods

Materials. The S-peptide-(1–19), residues 1–19 of RNase A, was kindly provided by Dr. Robert L. Baldwin. The sample contained some residual S-peptide-(1–20). 2,2,2-Trifluoroethanol-d_3 (99.4 atom % D) was purchased from MSD Isotopes. The other chemicals were of reagent grade and were used without further purification. All water was deionized and quartz distilled.

Samples were made up at a concentration of 2 mM S-peptide and contained 0.1 M NaCl and 0.01 M HCl or DCl. The solvent consisted of either H_2O containing 10% D_2O or of 99.8 atom % D_2O and contained 0, 5, 10, 15, or 20 mol % TFE-d_3. The samples contained TSP as an internal standard.

NMR Methods. NMR spectra were obtained on a Brüker AM-500 spectrometer. The temperature was controlled at 0 °C. The residual water proton signal in D_2O samples was suppressed by low-power irradiation during all periods except acquisition. Solvent suppression for samples in H_2O was achieved by higher power presaturation. Processing was done on a VAX 11-750 computer, using the program FTNMR written by Dr. Dennis Hare.

DQF-COSY spectra were obtained with time-proportional phase increments (TPPI) for phase-sensitive detection in F_2 (Marion & Wüthrich, 1983; Rance et al., 1983). A total of 512 FIDs of 32 scans each were collected, 4K Brüker points per FID (corresponding to 2K complex points), a sweep width of 5000 Hz, and a 2.5-s recycle delay being used. The carrier frequency was placed on the H_2O or residual HOD peak to minimize quadrature images. Processing was done by utilizing a 45° shifted sine bell apodization in the t_2 transform and a cosine bell in the t_1 transform, with zero filling in t_1 to a size of 2048 complex points, resulting in a square matrix of 2048 × 2048 complex points. These apodizations gave the best line shape in F_2 and the lowest ringing in the crosspeaks in the F_1 dimension. Since we are using low-power irradiation of the water resonance during t_1, it is possible to get Bloch–Siegert shifts in the F_1 dimension, resulting in erroneous chemical shifts (Wider et al., 1983). In D_2O solutions, the irradiation power is low enough that we do not observe any such shifts, as observed by a lack of deflection of the diagonal at the irradiation frequency and the equivalence within experimental uncertainty of the chemical shifts of the C^α protons, whether measured along the F_1 or F_2 axis.

Phase-sensitive NOESY spectra in 10 mol % TFE-d_3 and 90:10 H_2O/D_2O were obtained by using TPPI (Bodenhausen et al., 1984). The same basic spectral parameters as for the DQF-COSY spectra were used, except for a 300-ms mixing time and a 2-s recycle delay. Processing parameters were similar to those used in the DQF-COSY spectra.

RELAY spectra in 10 mol % TFE-d_3 and 90:10 H_2O/D_2O were obtained by utilizing a non-phase-sensitive t_1 detection (Wagner, 1983), by placing the carrier on the low-field side of the spectrum, and utilizing a sweep width of 8064 Hz. A total of 512 FIDs of 32 scans each was collected, with 4K Brüker points per FID. A recycle delay of 2.25 s and a refocusing delay of 25 ms were utilized. Unshifted sine bell apodization was utilized in both dimensions prior to magnitude calculation.

The resonance assignments in 10 mol % TFE-d_3 were made by using the DQF-COSY and RELAY spectra to assign the resonances within a residue and utilizing the NOESY crosspeaks between adjacent amide protons to produce the sequential assignments in order to assign each residue to its position in the sequence.

One-dimensional spectra of 5 mM Ala_3 (Sigma) were taken on a Brüker AM-400 spectrometer, at 25 °C in 0.1 M NaCl/0.01 M DCl, with 0, 5, 10, 15, and 20 mol % TFE-d_3. The chemical shifts were referenced to internal TSP.

Results

The resonance assignments were made in 10 mol % TFE at 0 °C. The three serines could not be individually assigned and are labeled Ser-a, Ser-b, and Ser-c, arbitrarily from lower to higher field C^α proton resonances in the absence of TFE. Figure 1 shows the DQF-COSY spectrum under these conditions, with the crosspeak identities labeled. The portion of the NOESY spectrum showing the crosspeaks from neighboring amide protons is shown in Figure 2, with several connectivities shown. NMR spectra taken on a Brüker AM-400 spectrometer at 25 °C were also used to confirm the assignments (data not shown).

The results of the TFE titrations are shown in Figures 3 and 4 for the C^α, C^β, C^γ, and side-chain ring protons. In addition, the titration curves for the C^α and C^β protons of the Ala_3 tripeptide at 25 °C are also shown in Figure 3 as a model for a random coil. No attempt was made to assign the Ala_3 resonances.

The Ala_3 tripeptide chemical shifts show a small downfield shift of approximately 0.04–0.07 ppm for all of the C^α and C^β protons. These same small shifts are observed for the C^α and C^β protons for Lys-1, Glu-2, Ser-a, Ser-b, Ser-c, Thr-17, and Ala-19. (The three serines could not be individually assigned.) On the other hand, the C^α and C^β protons of residues from Thr-3 to Met-13 show much more substantial shifts between 0 and 10 mol % TFE and essentially level off thereafter. The C^α protons of these residues (except Thr-3) shift to higher field by about 0.06–0.25 ppm. Most of the C^β protons exhibit a downfield shift, the opposite of the C^α protons. The main exception is His-12: one of the C^β protons shifts to higher field by approximately 0.22 ppm, while the other exhibits a much smaller 0.03 ppm shift to lower field. Asp-14 shows a small shift for the C^α and C^β protons, starting at 5 mol % TFE and leveling off at about 15 mol %.

The C^γ protons also exhibit shifts for residues between Thr-3 and Met-13, whereas Lys-1, Glu-2, and Thr-17 exhibit very small downfield shifts of approximately 0.04–0.06 ppm. Fi-

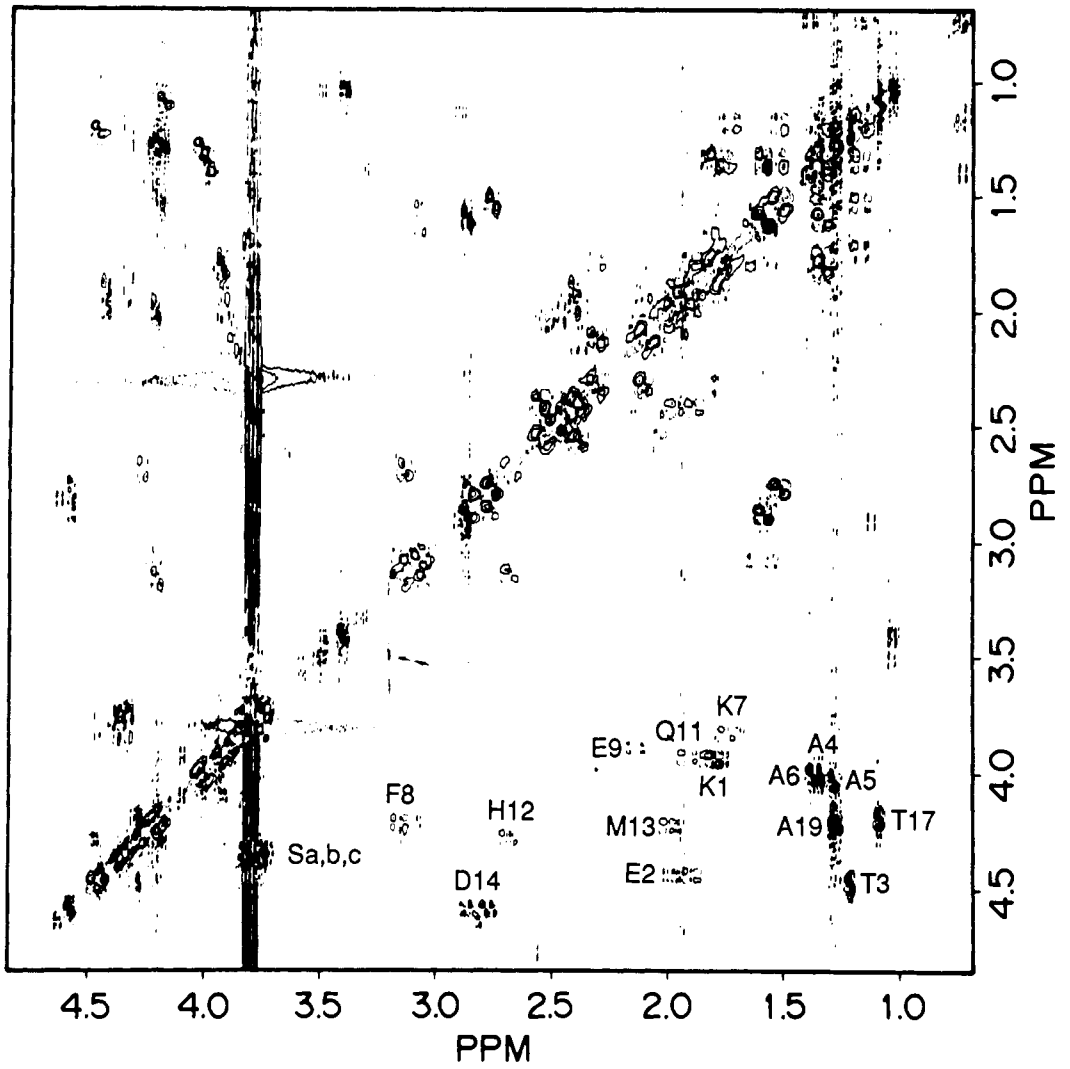

FIGURE 1: 500-MHz DQF-COSY spectrum of the S-peptide at 0 °C, in 10 mol % TFE-d_3, 0.1 M NaCl, 0.01 M DCl, and D_2O. Both positive and negative contours are shown. The vertical tracks near 3.8 ppm are due to the residual protons in the deuterated TFE. The acquisition and processing parameters are described in the text. The identities of the $C^{\alpha}H$ to $C^{\beta}H$ crosspeaks ($C^{\beta}H$ to $C^{\gamma}H$ for threonines) are labeled. The sample also contained some residual S-peptide-(1–20), which has Ala in position 20. This gives rise to the complexity of the Ala-19 crosspeak. The sequence of S-peptide-(1–19) is Lys-Glu-Thr-Ala-Ala-Ala-Lys-Phe-Glu-Arg-Gln-His-Met-Asp-Ser-Ser-Thr-Ser-Ala.

nally, the ring protons on Phe-8 and His-12 exhibit upfield shifts of between 0.1 and 0.5 ppm.

By examining the data in Figures 3 and 4, we can analyze some criteria for classifying residues that are induced to go helical. Small chemical shift changes of approximately 0.04–0.07 ppm to lower field for the C^{α}, C^{β}, and C^{γ} protons appear to indicate that a residue is not undergoing a significant helical transition. Changes in the C^{α} proton chemical shifts to higher field appear to indicate the formation of helical structure in those residues. An exception is Thr-3, which shifts downfield. The C^{β} protons show more diverse effects. Most shift to lower field, although in some cases the two geminal C^{β} protons shift to different extents or even in opposite directions. These unequal shifts are useful in indicating α-helix formation. The C^{γ} protons show similar effects as the C^{β} protons, although the chemical shifts move at higher TFE concentrations than those of the corresponding C^{β} protons for Lys-7 and Gln-11. The sensitivity is also low for the C^{γ} protons of Thr-3 and Met-13, which exhibit small downfield shifts of approximately 0.08 ppm. Thus, the C^{γ} protons are less useful for indicating α-helix formation. Protons further out than C^{γ} exhibited very little change in chemical shift with increasing TFE (data not shown). The ring protons on Phe-8 and His-12 exhibit shifts to higher field. In fact, the C2 proton on His-12 exhibits the largest shift of any proton, 0.48 ppm. This large change might be due to interactions with the aromatic ring of Phe-8, with the large ring current of the Phe-8 affecting the His-12 ring protons. Such an interaction between Phe-8 and His-12 has been postulated (Rico et al., 1986). We have no information on how much each residue's proton chemical shift changes when it becomes helical. Thus, we cannot correlate the extent of the shift with the extent of helical structure. We might expect that this shift will be different for each amino acid.

We are confident that the measured chemical shift changes indicate the formation of α-helical structure. This is based on the corroboration of the TFE titration of S-peptide measured by NMR and CD (Nelson & Kallenbach, 1986) and the denaturation by urea or guanidinium chloride measured by NMR and CD (Kim & Baldwin, 1984). In addition, the NOESY crosspeaks due to sequential amide protons are indicative of α-helix formation.

The chemical shift titrations of the C^{α}, C^{β}, C^{γ}, and ring protons seem to indicate that residues Thr-3 through Met-13 are undergoing a transition to α-helix up to about 10 mol % TFE. The chemical shifts then level off. Asp-14 seems to be an exception to this: it exhibits little change between 0 and 5 mol % TFE and then shifts between about 5 and 15 mol %

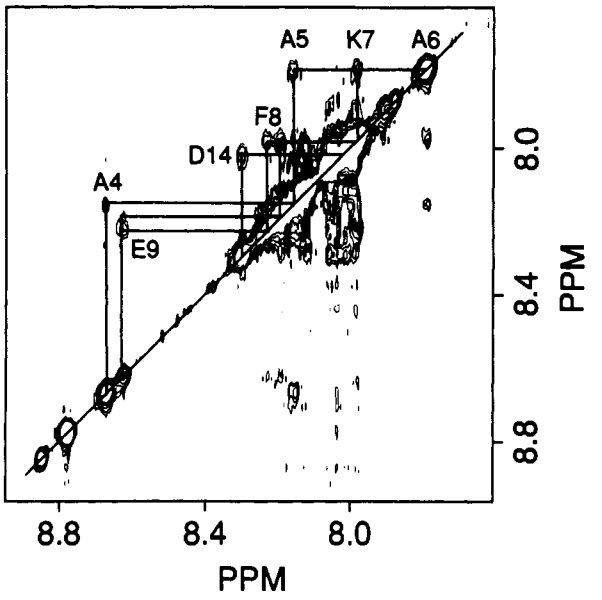

FIGURE 2: 500-MHz phase-sensitive NOESY spectrum of the S-peptide at 0 °C, in 10 mol % TFE-d_3, 0.1 M NaCl, and 0.01 M HCl, in 90:10 H_2O/D_2O. The crosspeaks arising from sequential NOE's from amide protons of Ala-4 through Glu-9 are labeled according to the proton's chemical shift on the horizontal (F_2) axis. The crosspeak immediately to the right of that labeled Phe-8 corresponds to the crosspeak from Arg-10 to Gln-11 and is unlabeled to avoid crowding. The crosspeaks connecting Gln-11, His-12, and Met-13 are too close to the diagonal to resolve. The last sequential crosspeak corresponds to that of Met-13 to Asp-14. The acquisition and processing parameters are described in the text.

TFE. This might indicate that the helix stops at Met-13 up to 5 mol % TFE, whereas it extends to Asp-14 at TFE concentrations between 5 and 15 mol %. Of course, our data cannot rule out a different conformational transition for Asp-14.

Discussion

High-resolution NMR methods make it possible to investigate specific residues in the S-peptide as the structure changes in the presence of TFE. Here we have measured the chemical shifts of nonexchangeable protons in the molecule to define the process of helix induction by TFE, a strong helix-stabilizing solvent (Nelson & Kallenbach, 1986). In the case of the S-peptide, Kim and Baldwin (1984) reported that the chemical shifts of several side chains between Thr-3 and His-12 respond to pH and urea or guanidinium chloride in parallel to changes in the CD spectrum, reported as the mean residue ellipticity at 222 nm, $[\theta]_{222}$. They could not determine the structure transition of Met-13. From their data, helix formation in the S-peptide is accompanied by detectable changes in the chemical shifts of a number of side chains as well as by alterations in $[\theta]_{222}$. While the origin of the chemical shifts in proteins is generally complex, helix formation in the isolated S-peptide is readily monitored by means of differences in these shifts.

TFE has two important functions in these experiments. We undertook the present work to determine the effects of TFE on the stability of α-helices. This stabilization has a very important consequence—it creates structure in an otherwise mostly unstructured peptide, enhancing the intensity of NOE crosspeaks between adjacent amide protons of the α-helix. This makes sequential assignment of the amide protons, and thus the entire NMR spectrum, possible. Extrapolation of each assigned resonance to zero TFE concentration results in unambiguous assignments for the molecule in aqueous solution. The only requirement for this application is that TFE must induce structure resulting in NOE interactions and that the chemical shifts can be followed at different TFE concentrations. Both requirements are met in the case of S-peptide.

In our previous study of the effect of TFE, we used $[\theta]_{222}$ to monitor the increased stability and extent of helical structure in the S-peptide (Nelson & Kallenbach, 1986). Given the dramatic increase in signal (increasingly negative value) at $[\theta]_{222}$ with increasing TFE concentrations, the question we raise here is whether or not the stop signal, which apparently blocks propagation of the nucleated α-helix near His-12, functions in the presence of TFE.

To place this question in a proper context, analysis of the helix-to-coil transition in synthetic "host" peptide copolymers incorporating different amino acids as guests revealed that nucleation of short α-helical segments is a highly unfavorable reaction (Sueki et al., 1984). In the notation of Zimm and Bragg (1959), the equilibrium constant K for forming a perfect helix of n identical residues can be approximated as

$$K = \sigma s^{n-3}$$

where σ is a nucleation constant and s is the stability constant for helix propagation. The synthetic polypeptide results suggest that $\sigma \simeq 10^{-4}$ regardless of the amino acid, while the s values characterizing propagation cluster around $s = 1$. This implies that helix formation with peptides of about 10–15 residues is unlikely. The "cooperative length", or average length of a helical segment, is $\sigma^{-1/2}$, or 100 residues for this model. Thus, once a helical region initiates, it should propagate over most of the residues in a short peptide.

The mechanism of helix stabilization by TFE, as we have discussed before, remains unknown. Since the dielectric constant of TFE is about one-third that of water, one would expect enhanced electrostatic interactions. We were thus surprised to find that the magnitude of the charged-group effect does not change significantly, even up to a concentration of 40 mol % TFE (Nelson & Kallenbach, 1986). Regardless of the mechanism, the consequence is a significant drop in $[\theta]_{222}$ consistent with increased α-helix content.

Inspection of the titration profiles in Figures 3 and 4 shows that, as in the case of the pH-dependent stability of the S-peptide α-helix in water, residues Thr-3 to Met-13 participate in the helix on the basis of changes in the chemical shifts of backbone C^α protons as well as C^β and C^γ side-chain protons, while the six residues C-terminal to Met-13 do not (although Asp-14 might increase its helicity between 5 and 15 mol % TFE). Interpreting the transition of the N-terminal residues is ambiguous due to the proximity to the end of the helix. Thus, we cannot distinguish helix termination at the N-terminus from fraying of the first two residues. The first process suggests an active mechanism to terminate the helix, whereas the second is a consequence of helix–coil transitions.

The NMR data provide limited information about the cooperativity of α-helix formation in TFE. The chemical shifts of residues Thr-3 through Met-13 start changing in concert as TFE is added, suggesting that the entire stretch is becoming helical together. However, since we do not know the chemical shifts for fully helical S-peptide under these conditions, we cannot say whether each residue is helical to the same extent. For example, the fraction of Phe-8 that is helical may differ from that of Thr-3 or Met-13. The observation that Asp-14 may be induced to go helical at higher TFE concentrations might suggest that the α-helix transition is not completely cooperative. The observation that the chemical shifts level off about 10 mol % TFE for the helical residues does not indicate that the residues are fully helical. TFE might induce only so much helicity up to 10 mol %, and further additions might not increase the helicity above this value.

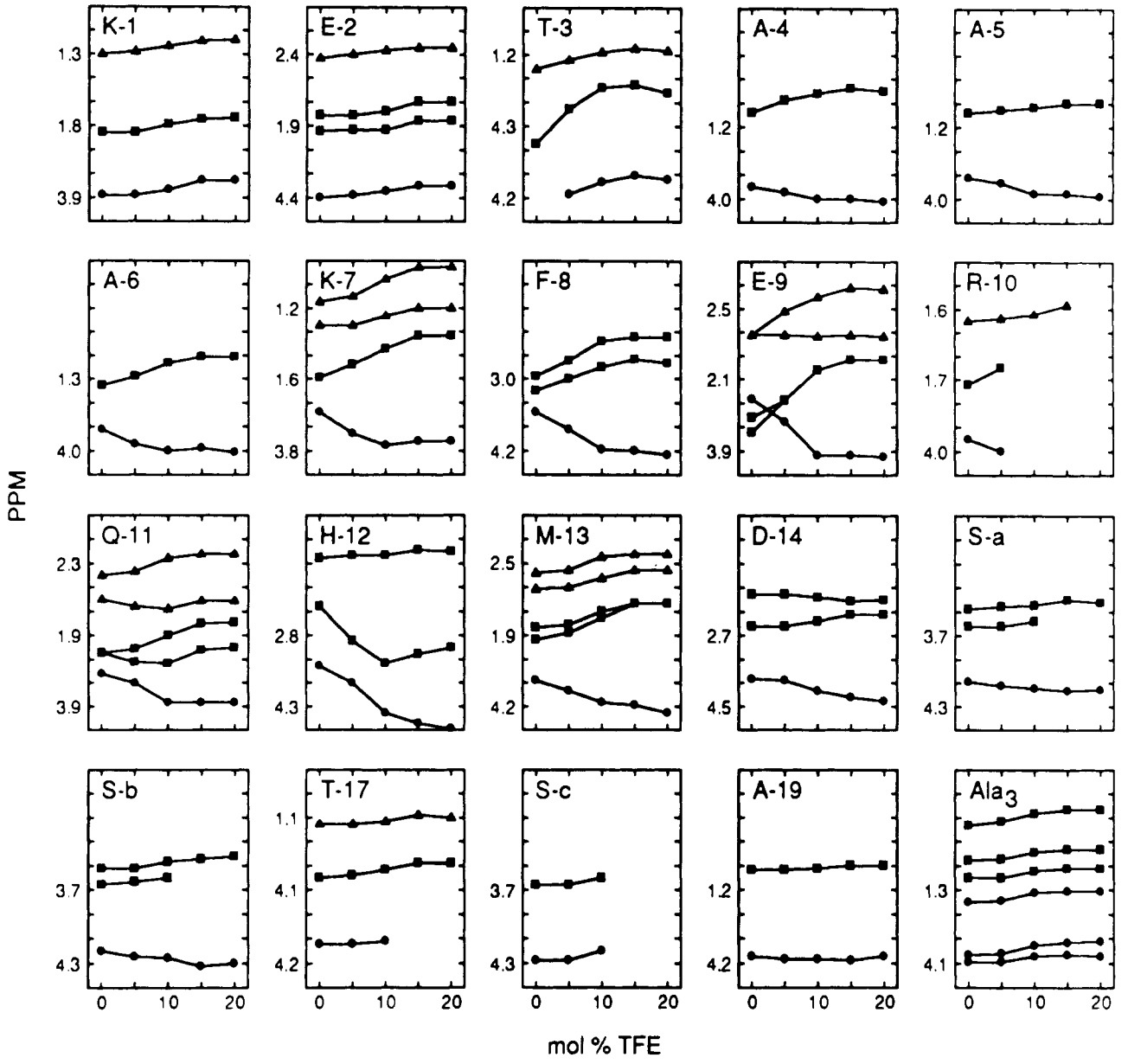

FIGURE 3: Plots of the chemical shift vs TFE concentration for the C^{α}, C^{β}, and C^{γ} protons of the S-peptide. The chemical shifts were measured from 500-MHz DQF-COSY spectra recorded at 0 °C in 0.1 M NaCl, 0.01 M DCl, and D_2O containing 0–20 mol % TFE-d_3. The vertical scale corresponds to 0.1 ppm per division for all protons. The C^{α} protons are plotted on the bottom (●), with the chemical shifts aligned to the axis by the lowest numeric label. The C^{β} protons (■) are in the middle, corresponding to the second label, and the C^{γ} protons (▲) are in the top third of each graph, corresponding to the uppermost label. For example, for Lys-1, the vertical axis for the C^{α} proton runs from 3.8 to 4.7 ppm; for the C^{β} protons, it runs from 1.4 to 2.3 ppm; and for the C^{γ} protons, it runs from 0.6 to 1.5 ppm. The three serines, labeled Ser-a, Ser-b, and Ser-c, could not be individually assigned. They are put into positions 15, 16, and 18 arbitrarily in alphabetical order. Plotted at the bottom right are the data for all the C^{α} and C^{β} protons of the tripeptide Ala_3 as a comparison of a random-coil model. Not all resonances could be followed throughout the titrations: Thr-3 and Thr-17 because of overlap of the C^{α} and C^{β} proton resonances, Arg-10 due to too low intensity of the broad crosspeak, and the serines because of overlap with the residual protons in TFE.

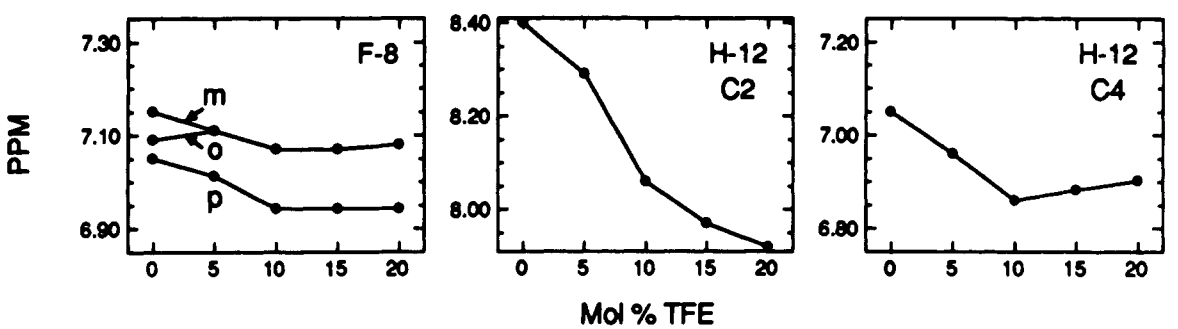

FIGURE 4: Plots of the chemical shift vs TFE concentration for the ring protons of Phe-8 and His-12 of the S-peptide.

We believe these results provide a clue to the functioning of the helix stop signal. Persistence of the stop signal in the perturbed environment represented by high concentrations of TFE suggests that the stop signal might be encoded in a direct

structural interaction. There are several possible candidates for the stop signal: the polar side chains of Ser or Asp might present competing H-bonding sites for the N—H···O=C donor–acceptor pairs of the α-helix backbone. This has been hypothesized as an important contribution for terminating helices early in the folding process (Presta & Rose, 1988). Alternatively, the involvement of two side chains in a specific interaction might prevent the elongation of the helix. In fact, it has recently been observed that a salt bridge between Glu-2 and Arg-10 in a peptide analogue of the first 13 residues of RNase A terminates the N-terminal end of the helix between Glu-2 and Thr-3 (John J. Osterhout, personal communication). These are only two of several possible interactions which might terminate helices. If these interactions are stabilized by TFE in concert with α-helix stabilization, the stop signal would be expected to remain intact in the presence of TFE.

ACKNOWLEDGMENTS

We thank Drs. Robert L. Baldwin and Peter S. Kim for providing the S-peptide samples and for many valuable discussions. The Brüker AM-500 NMR spectrometer at the Institute for Cancer Research in Philadelphia is supported by Instrument Grants RR 02497 (NIH) and DMB 84-13986 (NSF), by an award from Marie Z. Cole Montrose, by NIH Grants CA 06927 and RR 05539, and by an appropriation from the Commonwealth of Pennsylvania awarded to the Institute for Cancer Research. The Brüker AM-400 NMR spectrometer in the College of Basic Sciences at Louisiana State University was funded in part by NIH Shared Instrumentation Grant RR 02459.

Registry No. S-Peptide, 65742-22-5.

REFERENCES

Bodenhausen, G., Kogler, H., & Ernst, R. R. (1984) *J. Magn. Reson. 58*, 370–388.
Brown, J. E., & Klee, W. A. (1971) *Biochemistry 10*, 470–476.
Filippi, B., Borin, G., & Marchiori, F. (1976) *J. Mol. Biol. 106*, 315–324.
Filippi, B., Borin, G., Moretto, V., & Marchiori, F. (1978) *Biopolymers 17*, 2545–2559.
Kim, P. S., & Baldwin, R. L. (1984) *Nature 307*, 329–334.
Marion, D., & Wüthrich, K. (1983) *Biochem. Biophys. Res. Commun. 113*, 967–974.
Nelson, J. W., & Kallenbach, N. R. (1986) *Proteins 1*, 211–217.
Presta, L. G., & Rose, G. D. (1988) *Science 240*, 1632–1641.
Rance, M., Sørensen, O. W., Bodenhausen, G., Wagner, G., Ernst, R. R., & Wüthrich, K. (1983) *Biochem. Biophys. Res. Commun. 117*, 479–485.
Rico, M., Santoro, J., Bermejo, F. J., Herranz, J., Nieto, J. L., Gallego, E., & Jiménez, M. A. (1986) *Biopolymers 25*, 1031–1053.
Shoemaker, K. R., Kim, P. S., Brems, D. N., Marqusee, S., York, E. J., Chaiken, I. M., Stewart, J. M., & Baldwin, R. L. (1985) *Proc. Natl. Acad. Sci. U.S.A. 82*, 2349–2353.
Shoemaker, K. R., Kim, P. S., York, E. J., Stewart, J. M., & Baldwin, R. L. (1987) *Nature 326*, 563–567.
Sueki, M., Lee, S., Powers, S. P., Denton, J. B., Konishi, Y., & Scheraga, H. A. (1984) *Macromolecules 17*, 148–155.
Wagner, G. (1983) *J. Magn. Reson. 55*, 151–156.
Wider, G., Hosur, R. V., & Wüthrich, K. (1983) *J. Magn. Reson. 52*, 130–135.
Zimm, B. H., & Bragg, W. K. (1959) *J. Chem. Phys. 31*, 526–535.

^{1}H NMR Characterization of *Chromatium gracile* High-Potential Iron Protein and Its Ruthenium-Modified Derivatives. Modulation of the Reduction Potentials in Low- and High-Potential [Fe_4S_4] Ferredoxins†

M. Sola,‡ J. A. Cowan, and Harry B. Gray*
Arthur Amos Noyes Laboratory, California Institute of Technology, Pasadena, California 91125
Received October 19, 1988; Revised Manuscript Received February 17, 1989

ABSTRACT: The NMR spectra of the high-potential iron protein from the photosynthetic bacterium *Chromatium gracile* and its ruthenium-labeled (His-42 and His-20) derivatives are reported. The isotropically shifted resonances in both the oxidized and reduced forms show a complex pH dependence due to the presence of three ionizable residues (Glu-44, His-20, and His-42). Assignments have been made to specific residues and the spectral features compared to those of other bacterial HiPIP's. The decrease in the reduction potential with increasing pH for this class of proteins is attributed to stabilization of the oxidized state of the cluster by delocalization of electron density onto the neighboring Tyr-19 residue.

High-potential iron proteins (HiPIP's) are a class of enzymes containing [Fe_4S_4] clusters that possess large positive reduction potentials ($E°$ ranging from 100 to 350 mV) and are frequently found in photosynthetic bacteria, although one example has also been associated with a denitrifying bacterium (Palmer, 1975; Carter, 1977; Bartsch, 1978; Meyer et al., 1983). An electron-transport role has commonly been assumed, although there has been no conclusive evidence to support this belief. A related series of [Fe_4S_4] ferredoxins (Fd's) that contain a structurally identical prosthetic group differ in the cluster reduction potential, typically $E° \sim -400$ mV, and have led to much discussion concerning the factors

† Contribution No. 7872. This research was supported by the National Institutes of Health (DK-19038). J.A.C. thanks the Science and Engineering Research Council (United Kingdom) for a NATO Postdoctoral Fellowship.
‡ Present address: Department of Chemistry, University of Modena, Via Campi 183, 41100 Modena, Italy.

0006-2960/89/0428-5261$01.50/0